Journal of Microbiological Methods, 16 (1992) 47–58

MIMET 00513

Multi-electrode probe for statistical evaluation of microbiologically influenced corrosion

D.E. Nivens[a,b], R. Jack[b], A. Vass[b], J.B. Guckert[b], J.Q. Chambers[a] and D.C. White[b,c,d]

[a]*Department of Chemistry*, [b]*Center for Environmental Biotechnology, and* [c]*Department of Microbiology, University of Tennessee, Knoxville, TN, 37932, USA and* [d]*Environmental Science Division, Oak Ridge National Laboratory, Oak Ridge, TN 37831-6036, USA*

(Received 28 January 1992; accepted 10 April 1992)

Summary

Microbial biofilms increase the complexity and spatial variation of the interfacial chemistry occurring at metal surfaces and can facilitate corrosion. A multi-electrode probe was designed to replicate interfacial chemistry by providing multiple interfaces on a single probe. Electrochemical impedance spectroscopy (EIS) was used to examine the electrochemical properties of four-electrode probes containing 430 (USN430000) stainless steel coupons in test solutions. The EIS results obtained with the probe were compared to the ASTM G-106 standard method, and the probe was determined to be accurate. In addition, no interference or crosstalk between electrode channels was observed. In order to demonstrate the utility of the probe, four-electrode probes were used to investigate microbiologically influenced corrosion of C1020 carbon steel. Enrichments of aerobic, fermentative, and sulfate reducing bacteria from a corrosion tubercle were inoculated into the bulk phase of a corrosion cell and formed biofilms on the carbon steel electrodes. A five fold increase in the polarization admittance of carbon steel coupons exposed to biofilms relative to sterile medium was observed. The four-electrode probe provided the necessary degrees of freedom to show the statistically significant differences.

Key words: Microbiologically influenced corrosion; Multi-electrode; Statistics

Introduction

Microbiologically influenced corrosion (MIC) is recognized as a problem in a number of environmental and industrial settings [1,2]. Microorganisms attach to metal surfaces, such as ship hulls, metal pipes, support structures, and holding tanks, utilize solutes and adsorbates as nutrients, secrete extracellular polymers, and form metabolically active biofilms [3]. Biofilms are dynamic entities that are spatially heterogeneous and can involve many different interacting microbial species [4]. The heterogeneous distribution and diversity of microorganisms produce biofilms

Correspondence to: D.E. Nivens, 10515 Research Drive, Bldg 1, Suite 300, Knoxville, TN 37932, USA.

which vary in thickness, density [5], and specific metabolic activity [6,7]. These spatial variations affect the concentrations of solutes and metabolites at specific sites on a given surface. Thus microorganisms, working alone or synergistically, create micro-environments that alter the localized interfacial chemistry which, in turn, can facilitate corrosion [1,8–10]. The variation in biological parameters affects the variability in data that is used to evaluate MIC. Proper replication and statistical treatment should be used in MIC studies as shown by Denenberg who examined statistical considerations in biological systems [11], and Boffardi and Godard who discussed the practical use of statistics in corrosion experiments [12].

Electrochemical techniques are used to study corrosion phenomena. Classical corrosion studies utilized linear polarizations to obtain Tafel values and polarization resistances (R_p) to calculate corrosion rates [13]. However, it is generally accepted that techniques involving large current densities such as linear polarizations damage biofilms. Techniques in which the current density is small such as the measurement of open circuit potential (OCP), electrochemical noise, electrochemical impedance spectroscopy (EIS), and small amplitude cyclic voltammetry are used to monitor MIC [14]. EIS is a powerful tool for characterizing electrochemical properties of materials and interfaces by measuring parameters such as relaxation times (ω_o) double layer capacitance, inductance, solution resistance (R_Ω) and polarization resistance (R_p) [15–17]. Dowling et al. used both EIS and linear polarization to study MIC [18]. In addition, Franklin et al. showed that the small current densities generated by impedance measurements did not damage biofilms [19].

MIC hypothesis testing generally involves exposure of several metal samples of similar composition to sterile and microbial treatments. In order to replicate the biofilm/electrode interface and simplify experimental design, a multi-electrode probe has been designed. This probe allows for the independent replication of the MIC/surface interaction, not merely at the level of the probe analysis, but also at the level of an individual electrode interface on a probe. For this study, four-electrode probes were fabricated. This paper (1) describes the fabrication process, (2) investigates the accuracy of the probe at the electrode interface and probe level, and (3) demonstrates its utility in a MIC experiment by showing a statistically significant difference between sterile and microbial treatments.

Materials and Methods

Construction of a multi-electrode probe

Test probes were produced by mounting 1.6 cm diameter metal coupons (Metal Samples Inc., Munford, AL) onto a Teflon mold and embedding them in epoxy (ACME Chemicals & Insulation Co., New Haven, CT). The mold, constructed from a 5.1 cm diameter and 2.2 cm long Teflon cylinder, was used to give the multi-electrode probe its shape. For a four-electrode probe (Fig. 1), a square hole in the mold was required. This was achieved by cutting the cylinder in half and removing a right triangular section from each half of the cylinder. Wires were soldered onto the back of the metal coupons to provide the electrical connection. The coupons were placed on each face of the square hole and temporarily held in position with rubber bands. A Teflon support ring was placed in the hole and wedged between the coupons

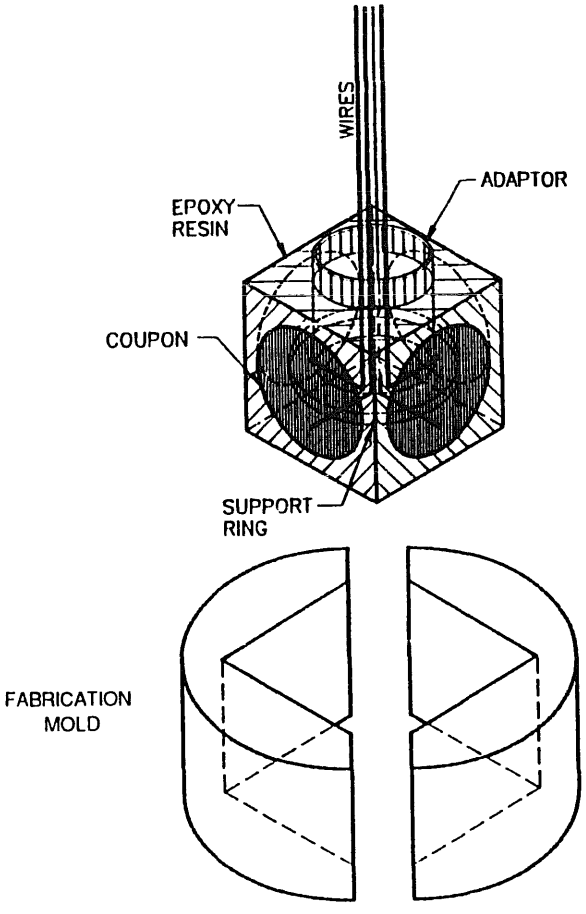

Fig. 1. Diagram of a four-electrode probe and its fabrication mold.

to secure them to the Teflon mold. Once the support ring was in place, a hose clamp was used to join the two halves of the cylinder together and the rubber bands were removed. The mold was mounted onto a flat glass or Teflon surface. Epoxy resin was added to the top of the mold and a Teflon adapter was immersed into the epoxy resin. Once the resin had hardened, each electrode was checked for continuity. The wires were fed through a glass tube inserted into the Teflon adaptor to protect the wires from the test solution.

Accuracy test

Test conditions. In order to test the accuracy of the four-electrode probe, the results of electrochemical impedance measurements were compared with the ASTM standard [20]. The test cell was a 1.5 l glass reaction vessel equipped with a polypropylene top and operated in a typical three electrode arrangement. The reference electrode was a saturated calomel electrode (SCE) isolated by a bridge tube. The counter electrode was constructed from titanium wire welded to a sheet of titanium that was bent into a U-shape to promote uniform current densities on the working electrode. The working electrode was the four-electrode test probe equipped with 1.6 cm diameter 430 (UNS430000) stainless steel coupons. Each experiment was performed in a 0.495 M Na_2SO_4 solution containing 5.0×10^{-3} M H_2SO_4. The tests

were carried out at room temperature (23 ± 2°C). All chemicals were reagent grade and all solutions were prepared with 18 MΩ-cm water. The working electrodes were wet polished with 600 grit silicon carbide paper, rinsed with 18 MΩ-cm water, degreased with ethanol, and immersed into the test solution within 1 h after polishing. Prior to test specimen immersion, the solution was purged for 1 h with N_2 to remove oxygen from the cell. Before electrochemical analysis, each electrode was turned and aligned in front of the reference electrode bridge tube. The titanium counter electrode was placed in front of the working electrode and directly behind the bridge tube.

Electrochemical impedance analysis. Impedance measurements were performed with an EG&G 273 potentiostat outfitted with option 92 and a Schlumberger 1255 frequency response analyzer (FRA). The data were collected by a personal computer using Z-plot software (Scribner Associates Inc., Charlottesville, VA). The open circuit potential was monitored for 1 h prior to the start of the experiment. The frequency response between 10000 Hz and 0.1 Hz was recorded at 10 steps per decade intervals. The root mean square amplitude of the input signal was 10 mV.

The impedance data was analyzed using Z-plot software. This software determines the best fit semicircle for the data presented in the complex plane plots. The polarization resistance (R_p) was estimated by the diameter of the semicircle. The solution resistance value (R_Ω) was estimated to be the point near the origin where the semicircle intersected the real impedance axis. The maximum angular frequency (f_o) is equal to the inverse of the relaxation time and was obtained by locating the frequency that led to the maximum value for the imaginary impedance component in each semicircle.

Statistical analysis. Twelve 430 stainless steel coupons were randomly assigned to three test probes, each probe containing four coupons. Impedance analysis was performed five times on each electrode. The electrodes were analyzed sequentially. A nested a priori test for analysis of variance (ANOVA) was performed to determine if a significant difference at the 95% confidence limits ($p \leqslant 0.05$) occurs between the probes or within the electrodes on each probe. The ANOVA analyses were performed with Minitab software.

Cross talk experiments

These experiments were performed with the same test system as the accuracy experiments, except an additional reference electrode bridge tube was added to the cell. A Schlumberger 7081 voltmeter was used to measure the OCP of an electrode adjacent to the electrode on the same probe subjected to an alternating potential signal. The alternating voltage input signal was ten cycles at 3×10^{-3} Hz with an amplitude of 10 mV.

MIC test conditions

Preparation of microbial enrichments. A tubercle from a carbon steel pipe was used as an inoculum to enrich for aerobic, fermentative and sulfate reducing communities. The pipe had been used to transfer estuarine cooling water for a hydroelectric power plant. Corrosion products from the tubercle were aseptically transferred to a test

tube containing 10 ml of medium consisting of 2 $g \cdot l^{-1}$ glucose, 2 $g \cdot l^{-1}$ sodium lactate, 0.5 $g \cdot l^{-1}$ NH_4Cl, 0.1 $g \cdot l^{-1}$ KH_2PO_4, and 1 $g \cdot l^{-1}$ $MgSO_4 \cdot 7H_2O$. This solution of medium and corrosion products was then inoculated into three different types of media designed to enrich for aerobic, fermentative, and sulfate reducing consortia. Each enrichment was then transferred and incubated in fresh medium prior to the start of the experiment. These enrichment procedures and media have been described in detail elsewhere [9]. Prior to inoculation, all enrichments were centrifuged for 20 min at 8000 × *g*. The supernatant was decanted and 10 ml of reduced mineral salts were added, vortexed and centrifuged. The microorganisms were washed three times by this procedure to remove all metabolites and/or products of microbial metabolism. The electrochemical cell was inoculated with 20 ml of each enrichment culture.

MIC test system. A continuous flow system was used to avoid an accumulation of corrosion products and microbial metabolites in the bulk phase. The flow system consisted of a medium reservoir, silicone tubing, two pumps, two electrochemical cells, and exit reservoirs. The medium contained 50 $mg \cdot l^{-1}$ glucose, 50 $mg \cdot l^{-1}$ sodium lactate, 5 $mg \cdot l^{-1}$ KH_2PO_4, 15 $mg \cdot l^{-1}$ NH_4Cl, and 80 $mg \cdot l^{-1}$ $MgSO_4 \cdot 7H_2O$. The flow rate was 1 $ml \cdot min^{-1}$. The electrochemical cell consisted of a 1 l reaction flask, an o-ring and a polypropylene top. Each cell contained an inlet drip tube, an exit line, a four-electrode probe with C1020 carbon steel coupons as working electrodes, a titanium counter electrode, a SCE reference electrode and bridge tube, an inoculation port, and a stir bar. The epoxy/coupon edge was covered with a lacquer (Microshield, Pyramid Plastics, Hope, AK) to help prevent crevice corrosion. The exit line was adjusted so that the total volume in each flask was 550 ml. The flow system was sterilized in an autoclave (121°C and 20 PSI for 20 min) except for the electrochemical cells which were sterilized with ethylene oxide to avoid the corrosion that occurs during steam sterilization. The medium was sterilized by filtration (0.2 μm pore diameter). The experimental electrochemical cells were inoculated with the three enrichment cultures to initiate the experiment, while the control flasks remained sterile. Prior to electrochemical analysis, the counter electrodes were repositioned away from the four-electrode probe in order to avoid blocking convectional currents during biofilm growth. Each working electrode was rotated so that it faced the bridge tube during the analysis.

Results

Accuracy test

The range of results for R_p values from the 60 impedance analyses of the electrodes for the three probes are represented by the solid and dashed lines in Fig. 2. The range of results for the ASTM G-106 standard method is presented as a shaded region (Fig. 2). The data are plotted in three different formats. Fig. 2A is a complex plane plot of the real impedance versus the negative of the imaginary impedance. Fig. 2B, C are Bode diagrams in which the log of the frequency is plotted versus the log of the impedance (Fig. 2B) and the log of the phase angle (Fig. 2C). These three standard plotting formats are used to observe and characterize electrochemical parameters of

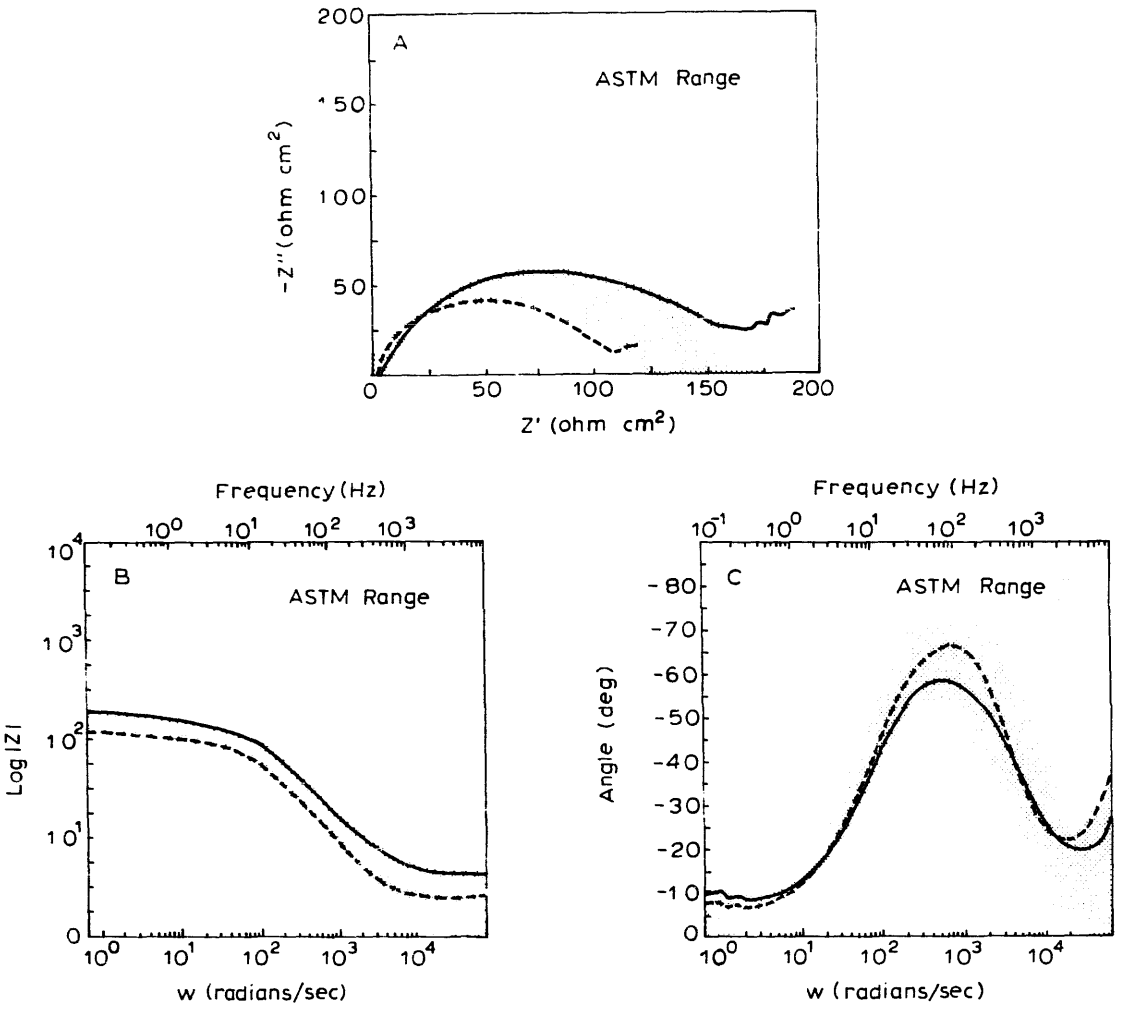

Fig. 2. Accuracy test data showing the range of the impedance data. Plot A is a complex plane diagram, plotting the real impedance versus the negative of the imaginary impedance. Plots B and C are Bode diagrams, plotting the log of the frequency versus the phase angle (B) and the log of the impedance (C).

corroding surfaces [17]. Of 60 analyses, 56 proved to be within the accuracy range, while the four other analyses from electrodes immersed for longer times produced results which were similar but slightly outside the ASTM standards (Fig. 2A). The corrosion potential (E_{corr}) ranged from -646 mV to -637 mV, which is within the ASTM prescribed interval (-645 ± 10 mV) [20].

The results from the nested analysis of variance (ANOVA) for E_{corr} and f_o showed that there was a significant difference between probes, but not between electrodes on a probe (Table 1). However, the statistical analysis of the R_p data demonstrated that there is a statistically significant difference between both test probes and between the different electrodes on each probe (Table 1). Statistically significant differences at the 95% confidence limits for probes and electrodes on a given probe are summarized in Table 1. A posteriori statistical tests showed that the values of E_{corr} and R_p correlated with time, where the correlation coefficients were 0.706 and -0.543 ($p \leqslant 0.01$), respectively. Fig. 3 presents R_p values plotted versus time for all the analyses on

TABLE 1

Statistically significant difference at 95% confidence limits ($p > 0.05$)

Variable	Between probes	Electrodes on a probe
E_{corr}	+	–
f_o	+	–
R_p	+	+

each probe, showing the negative correlation with time. Time zero in Fig. 3 indicates the onset of the impedance experiment. For Probe A, linear regression analyses yielded slopes of -2.7×10^{-3} ($r^2 = 0.915$), -2.9×10^{-3} ($r^2 = 0.988$), -2.7×10^{-3} ($r^2 = 0.982$) and -2.7×10^{-3} ($r^2 = 0.934$) $\Omega \cdot cm^2 \cdot s^{-1}$ for electrodes 1 through 4, respectively. For this probe, electrodes 2 and 3 decreased linearly, while electrodes 1 and 4 asymptotically approached a R_p value of approximately 120 $\Omega \cdot cm^2$. For Probe B, the data asymptotically approached R_p values which ranged between 117 and 124 $\Omega \cdot cm^2$. Similarly, probe C asymptotically approached R_p values which ranged between 108 and 122 $\Omega \cdot cm^2$. These data, when combined with the fact that the exposure time was greatest for probe C and least for probe A (A < B < C), suggests that short immersion times (probe A) led to measured R_p values which are similar to the estimates of the highest values for R_p from the ASTM data. Conversely, longer exposure times tended to yield R_p values for electrodes that are similar to the smallest values for R_p as estimated from the ASTM standard range. Assuming that the Tafel behavior remains constant [13], the measured R_p values are inversely proportional to the corrosion rate, thus smaller R_p values measured at longer immersion times equate to faster corrosion rates.

Crosstalk experiment

In the crosstalk experiments, an alternating voltage was applied to one of the electrodes while the potential was monitored on an adjacent electrode (Fig. 4). The alternating voltage input signal, a sine-wave with a frequency of 3 mHz and amplitude of 10 mV (rms), is represented by a dotted line in Fig. 4. After 50 min, the input signal was terminated. Qualitatively, the OCP signal (solid line) neither developed a sine-wave pattern when the input signal was activated nor changed its pattern after the signal was terminated. Quantitatively, the OCP data were fast Fourier transformed and the contribution of the 3×10^{-3} Hz component did not significantly contribute to the waveform.

MIC test

The multi-electrode probes were exposed to sterile medium and to aerobic, fermentative and sulfate reducing bacteria present in the enrichments. The OCP was used to signal the formation of a biofilm (Fig. 5). Two electrodes on each probe were monitored. The sterile control cell immediately stabilized at −250 mV versus SCE, while the OCP data of the electrochemical cell inoculated with the enrichments started to decrease at 30 h after inoculation and stabilized after 80 h at −700 mV versus SCE. At approximately 80 h, tubercles were observed on the surface of the

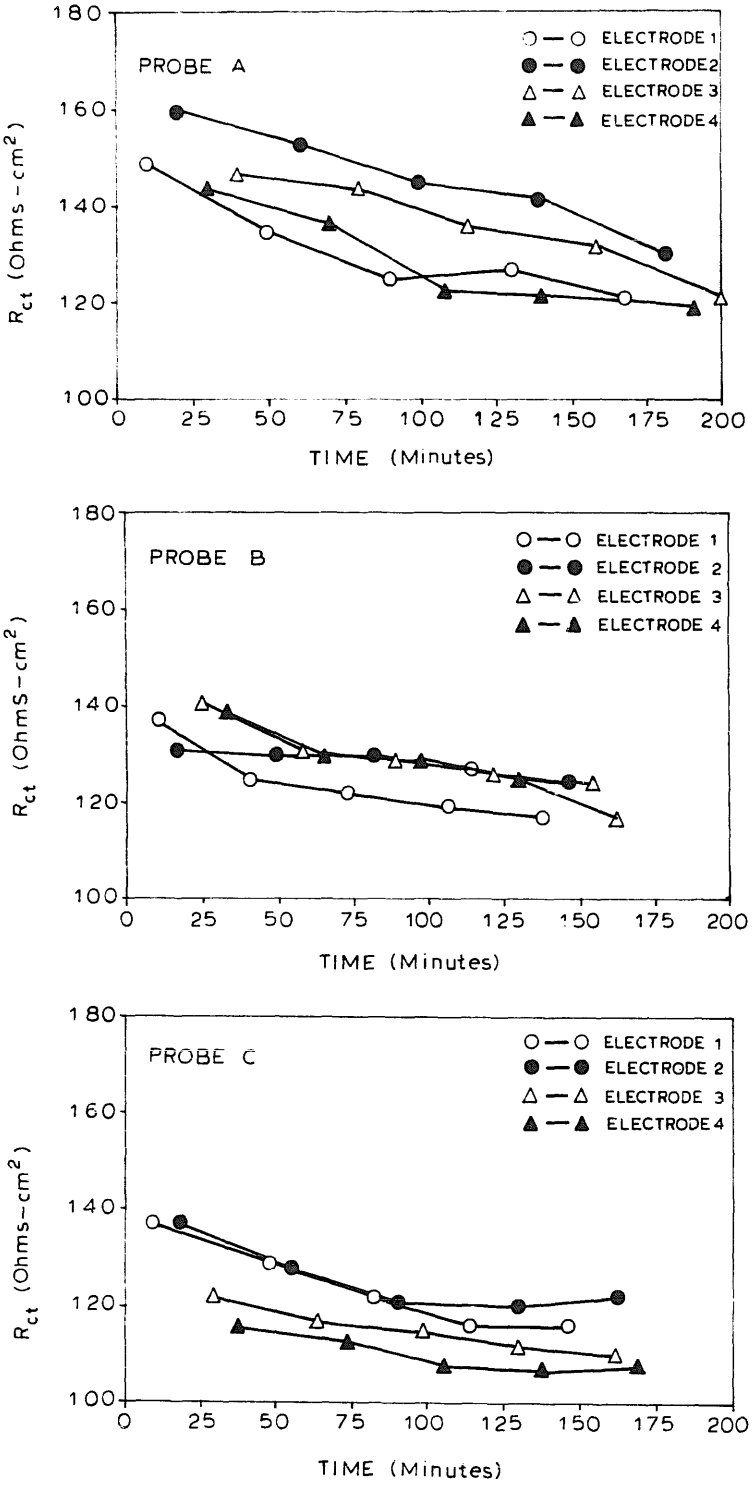

Fig. 3. Polarization resistance plotted versus time for all of the electrodes. Time zero is the start of the data collection and not the immersion time.

coupons. Impedance measurements were performed after 1, 5, 7, 9, 14, and 17 days. The mean and standard deviations of polarization admittance (R_p^{-1}) for the experimental flask and the sterile control at each time point is presented in Fig. 6. The

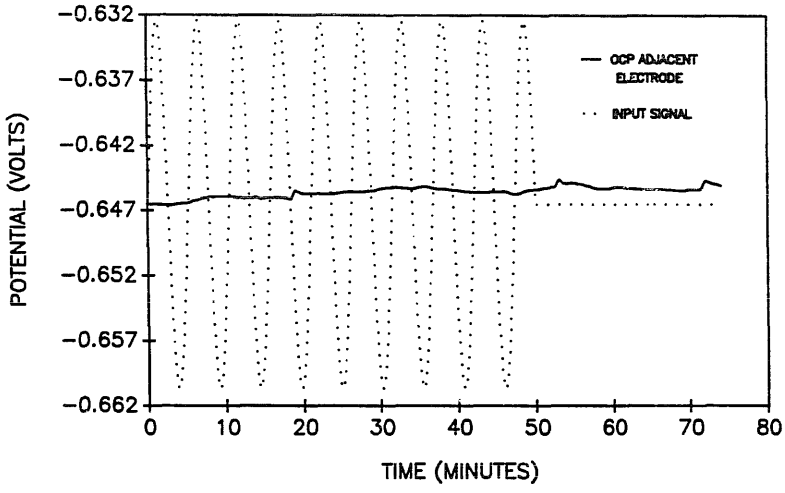

Fig. 4. Graph showing open circuit potential data during cross-talk experiment. The dashed line is the alternating voltage input signal (amplitude of 10 mV rms and a frequency of 0.0033 Hz) and the solid line shows the OCP data.

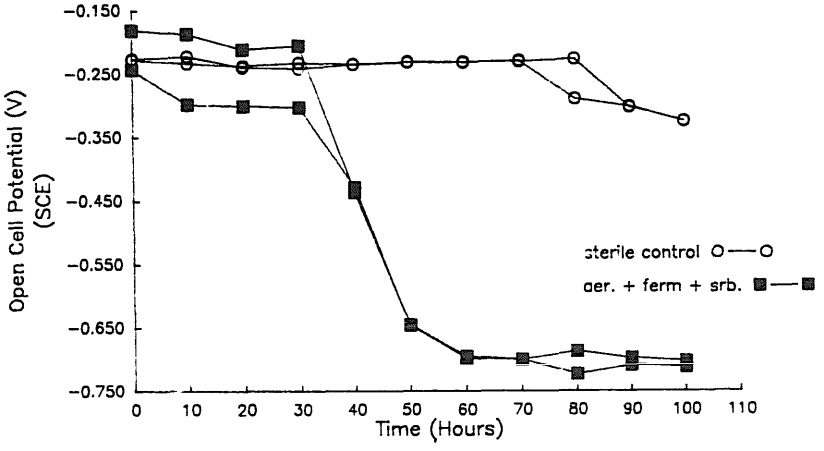

Fig. 5. OCP versus time for two electrodes on a probe for sterile and microbial treatments. Probes were exposed to sterile medium (open circles) and the aerobic, fermentative, and sulfate reducing bacterial enrichments.

admittance (Y_p) was plotted instead of the R_p, since Y_p is proportional to the corrosion rate assuming the Tafel behavior remained constant. After the initial time point, the experimental admittance data were significantly higher than the sterile control at the 95% confidence level (Student's t-test, $n=3$). The presence of the biofilm was verified by total plate counts, most probable numbers and total phospholipid fatty acid assays at the end of the experiment [9]. The control experiment remained sterile for the duration of the experiment.

Discussion

The multi-electrode probe simplifies experimental design by successfully combining four independent electrodes into a single probe. This probe is equivalent to four

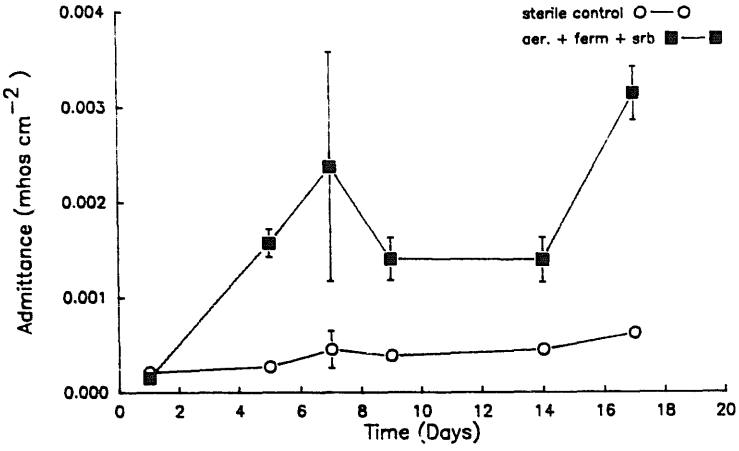

Fig. 6. Polarization admittance data at specific times for a sterile electrochemical cell and a cell inoculated with aerobic, fermentative, and sulphate reducing bacterial enrichments.

electrodes immersed in the same solution and can be used to replicate the chemistry occurring at the electrode/solution interface. The probe can be repolished and reused several times. Although the probe can be used to study any phenomenon transpiring at the electrode surface, it is especially useful in MIC studies where biofilms complicate the interfacial chemistry.

The accuracy test established that the four-electrode probe can be used to provide accurate results for EIS analyses and does not introduce any bias into the electrochemical measurements. However, ANOVA analysis determined that the probes and, for the case of R_p, the electrodes on a given probe are statistically different. The differences in measured R_p for electrodes on a given probe is probably related to the corrosion rate. The differences in the corrosion rates could be caused by metallurgical inhomogeneities such as MnS inclusions and/or crevice corrosion at the metal/epoxy interface. The ASTM protocol does not require that the epoxy/electrode interface be protected. The statistical differences between probes can be attributed to the types of variability associated with the probes and the high degree of replication involved with this experiment. Variability between probes contained not only the variability associated with the electrodes, but also variability related to differences in solute concentrations, temperature, immersion time and the degree of probe passivation. These results highlight the ability of the probe to examine variability at the electrode interface and probe level.

The crosstalk experiment demonstrated that the current densities generated by the impedance analysis did not induce a measurable effect on the other electrodes of the probe (Fig. 4). This result allows an investigator to perform impedance measurements on one electrode while simultaneously monitoring OCP on another. Other electrochemical techniques which apply little or no current density can be used to generate simultaneous electrochemical data.

The complex consortia of microorganisms isolated from a tubercle formed microbial biofilms on test surfaces and produced tubercles which were visually similar to the original tubercle. The formation of the biofilm also effected the OCP. Microorganisms can effect the redox potential by changing the interfacial concentration of

solutes such as oxygen [21], hydrogen ion (pH) [21] and/or sulfide ion [22] at the metal/biofilm interface. Fermentative bacteria produce short chain fatty acids that effect the pH, which in turn effect the OCP and may increase corrosion rates. Constituents of the aerobic enrichment utilize O_2 thus effecting the O_2 concentration which decreases the OCP and creates anaerobic microenvironments. Sulfate reducing bacteria growing in these microenvironments can lower the pH and produce aggressive sulfide ions that can facilitate corrosion [22]. The biofilm microorganisms not only affected the OCP, but also the R_p of C1020 mild steel coupons. The impedance data demonstrated that the admittance values were 5-fold higher for electrochemical cells inoculated with bacteria ($p \leqslant 0.05$) as compared to sterile controls. The four-electrode probe was used to provide the necessary degrees of freedom to prove statistically significant differences.

Acknowledgements

This research was supported by an Office of Navy Research Grant (N00014-88-K-0177), an NSF Grant (CHE-8718-057), the Science Alliance Program of the University of Tennessee, and the Environmental Science Division of Oak Ridge National Laboratory. The authors would like to thank Patty Hanna, David Ringelberg, Mike Franklin, and Marc Mittelman for their respective contributions.

References

1 Dowling, N.J.E., Mittelman, M.W. and White, D.C. (1991) Role of consortia in microbially influenced corrosion. In: Consortia in Biotechnology (Zeikus, G.J., Ed.), pp. 341–372, McGraw-Hill, New York, NY.
2 Franklin, M.J. and White, D.C. (1991) Biocorrosion, Cur. Biol. 2, 450–456.
3 Costerton, J.W., Cheng, K.J., Geesey, G.G., Ladd, T.I., Nickel, J.C., Dasgupta, M. and Marie, T.J. (1987) Bacterial biofilms in nature and disease, Anal. Rev. Microbiol. 41, 435.
4 Marshall, K.C. (1976) Interfaces in Microbial Ecology, p. 57 Harvard U. P., Cambridge, MA.
5 Christensen, B.E. and Characklis, W.G. (1990) Physical and Chemical Properties of Biofilms. In Biofilms (Characklis, W.G. and Marshall, K.C., Eds), p. 110, Wiley, New York, NY.
6 Mittelman, M.W., Nivens, D.E., Low, C. and White, D.C. (1990) Differential adhesion, activity, and carbohydrate: protein ratios of *Pseudomonas atlantica* monocultures attaching to stainless steel in a linear shear gradient. Microb Ecol. 19, p. 269.
7 Franklin, M.J., White, D.C. and Isaacs, H.S. (1991) Spatial and Temporal Relationships between Microbiological metabolism and Electrochemical Activity on Steel Surfaces. Paper no. 115, National Association of Corrosion Engineers, Cincinnati, OH.
8 Nivens, D.E., Nichols, P.D., Henson, J.M., Geesey, G.G. and White, D.C. (1986) Reversible acceleration of corrosion of stainless steel exposed to sea water induced by the extracellular secretions of the marine vibrio *V. natriegens*, Corrosion 42, 204.
9 Jack, R.F. (1990) The Effects of Increased Bacterial Metabolic Diversity on the Corrosion of Carbon Steel, Master's thesis, University of Tennessee.
10 Jack, R.F., Ringelberg, D.B. and White, D.C. (1991) The differential corrosion of carbon steel by combinations of *Bacillus* sp., *Hafnia alvei*, and *Desulfovibrio gigas established by phospholipid analysis of electrode biofilms*, Corrosion Sci. in press.
11 Denenberg, V.H. (1976) Statistics and Experimental Design for Behavioral and Biological Researchers, Wiley, New York, NY.
12 Boffardi, B.P. and Godard, H.P. (1990) Practical applications of statistics, Mater. Perform. 29, 87.
13 Stern, M. and Geary, A.L. (1958) Electrochemical polarization. I. A theoretical analysis of the shape

of polarization curves. J. Electrochem. Soc. 104, 56.
14 Mansfeld, F. and Little, B. (1990) The Application of Electrochemical Techniques for the Study of MIC - A Critical Review. Paper no. 108, National Association of Corrosion Engineers, Las Vegas, NV.
15 Mansfeld, F. (1981) Recording and analysis of AC impedance data for corrosion studies I. Background and method of analysis, Corrosion 36, 301.
16 Mansfeld, F., Kendig, M.W. and Tsai, S. (1982) Recording and analysis of AC impedance data for corrosion studies. II. Experimental results and approach, Corrosion 38, 570.
17 Macdonald, D.D. (1987) Theoretical analysis of electrochemical impedance. Paper no. 479, Corrosion 87, National Association of Corrosion Engineers, San Francisco, CA.
18 Dowling, N.J.E., Guezennec, J., Lemoine, M.L., Tunlid, A. and White, D.C. (1988) Corrosion analysis of carbon steels affected by aerobic and anaerobic bacteria in mono and co-cultures using AC impedance and DC techniques, Corrosion 44, 869.
19 Franklin, M.J., Nivens, D.E., Guckert, J.B. and White, D.C. (1991) Effect of electrochemical impedance spectroscopy on microbial cell numbers, viability, and activity, Corrosion 79, 519–522.
20 ASTM G-106 (1990) Standard Practice for Verification of Algorithm And Equipment for Electrochemical Impedance Measurements, p. 432, ASTM, Philadelphia, PA.
21 Lewandowski, Z., Lee, W.C., Characlis, W.G. and Little, B. (1988) Dissolved oxygen and pH microelectrode measurements at water immersed metal surfaces. Corrosion 88, paper no. 93, National Association of Corrosion Engineers, St. Louis, MO.
22 Hardy, J.A. and Brown J.L. (1984) The corrosion of mild steel by biogenic sulfide films exposed to air. Corrosion, 40, 650.